

ANALYTICAL MOMENT-CURVATURE RELATIONS FOR TIED CONCRETE COLUMNS

By Shamim A. Sheikh,¹ Member, ASCE, and C. C. Yeh²

ABSTRACT: The research reported here is a follow-up on experimental work in which 16 12 in. (305 mm) square and 9 ft (2.74 m) long columns were tested under flexure to large inelastic deformations while simultaneously subjected to axial load that remained constant throughout the test. The main variables included the distribution of longitudinal and lateral steel, amount of lateral steel, tie spacing, and axial load level. In this paper, the predictions for the behavior of these specimens from the available stress-strain models for confined concrete are compared with the test results. After a critical examination of the analytical models and the variables that affect the behavior of the specimens, a model originally proposed for concentric compression was modified to include the effects of strain gradient and the level of axial load. As a result of strain gradient, the concrete is able to sustain additional deformation at and beyond the peak stress. The effect of increased axial load is incorporated with reduced concrete strength. A numerical example is presented in which the use of a rectangular stress block representing the actual stress-strain curve of concrete obtained from the confinement model is demonstrated.

INTRODUCTION

Use of confining steel in the critical regions of columns designed for earthquake resistance is a common way of achieving ductile structural behavior. The lateral steel, in conjunction with the longitudinal steel, affects the concrete properties significantly depending on several factors, which include distribution of steel including spacing of longitudinal and lateral steel, amount of lateral steel, and the type of anchorage of lateral steel. In addition, the mobilization of concrete confinement is affected by the strain gradient caused by flexure. In general, a conservative evaluation of the capacity is considered safe. However, in the capacity design approach (Pau-lay 1980), for seismic considerations, an underestimation of flexural capacity may result in a brittle shear fracture even when the members are well-detailed for ductile flexural behavior.

The research reported in this paper is a follow-up of the experimental work reported recently (Sheikh and Yeh 1990; Yeh and Sheikh 1988). The analytical models for confined concrete available in the literature (Fafitis and Shah 1985; Mander et al. 1988; Park et al. 1982; Sheikh and Uzumeri 1982) were applied to predict the results of the present series of tests (Sheikh and Yeh 1990; Yeh and Sheikh 1988). The specimens reinforced with longitudinal steel and rectilinear ties were tested under flexure to large inelastic deformations while simultaneously subjected to constant axial loads. Moment capacities of the specimens were also compared with the theoretical nominal strength capacities obtained by using the ACI Code ("Building" 1989) procedure based on unconfined concrete strength.

¹Assoc. Prof., Dept. of Civ. Engrg., Univ. of Toronto, Ontario, Canada M5S 1A4.

²Formerly, Grad. Student, Dept. of Civ. Engrg., Univ. of Houston, Houston, TX 77204.

Note. Discussion open until July 1, 1992. To extend the closing date one month, a written request must be filed with the ASCE Manager of Journals. The manuscript for this paper was submitted for review and possible publication on June 4, 1991. This paper is part of the *Journal of Structural Engineering*, Vol. 118, No. 2, February, 1992. ©ASCE, ISSN 0733-9445/92/0002-0529/\$1.00 + \$.15 per page. Paper No. 26556.

A comparative study of the available confinement models was conducted earlier (Sheikh 1982) for their application to the specimens under concentric compression. It was observed in this study that in addition to the previously known variables that affect the behavior of confined concrete, the level of axial load also influences the properties of confined concrete significantly. An analytical model (Sheikh and Uzumeri 1982), which considers distribution of steel in addition to other commonly known factors predicted results better than other models, but did not adequately represent the effect of the level of axial load on the concrete behavior. This model was modified in the light of the test data.

ANALYTICAL MODELS

Modified Kent and Park (KP) Model

The original model was proposed by Kent and Park (1971) and modified by Park et al. (1982). In the original model, the ascending part of the stress-strain curve of concrete was considered to be unaffected by confinement. The slope of the descending part was a function of the amount of lateral steel and the ratio between core width and tie spacing. Park et al. (1982) modified the original model by making an allowance for the enhancement in the concrete strength and the peak strain due to confinement. The increase in concrete strength was assumed to be equal to $\rho_t f_{yh}$, where ρ_t is the volumetric ratio of tie steel, and f_{yh} is the yield strength of tie steel. The slope of the descending part of the curve remained the same as in the original model up to a stress of 20% of the maximum, beyond which a horizontal line represented the curve.

Sheikh and Uzumeri (SU) Model

This model (Sheikh and Uzumeri 1982) was developed based on the assumption that the effectively confined concrete area is less than the core area and is determined by the distribution of longitudinal steel, the resulting tie configuration and the spacing of ties. The model was calibrated against the results of the tests conducted on large-size specimens under concentric compression. Fig. 1 shows the proposed stress-strain curve OABCDE. The governing equations for a square section with uniform distribution of longitudinal steel bars are given as

$$f'_{cc} = K_s f_{cp} \dots \dots \dots (1)$$

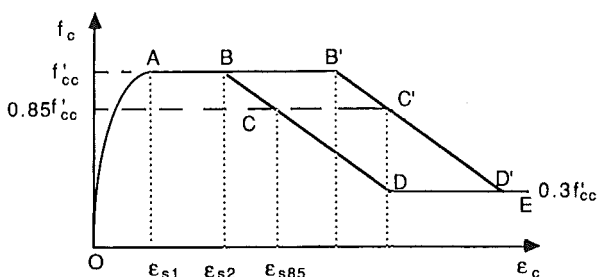


FIG. 1. Stress-Strain Models of Confined Concrete

$$K_s = 1.0 + \frac{B^2}{10.58P_{occ}} \left[\left(1 - \frac{nC^2}{5.5B^2}\right) \left(1 - \frac{s}{2B}\right)^2 \right] \sqrt{\rho_t f'_s} \dots \dots \dots (2)$$

$$\epsilon_{s1} = 0.55K_s f'_c (10^{-6}) \dots \dots \dots (3)$$

$$\frac{\epsilon_{s2}}{\epsilon_0} = 1 + \frac{0.81}{C} \left[1 - 5 \left(\frac{s}{B}\right)^2 \right] \frac{\rho_t f'_s}{\sqrt{f'_c}} \dots \dots \dots (4)$$

$$\epsilon_{s85} = 0.225\rho_t \sqrt{\frac{B}{s}} + \epsilon_{s2} \dots \dots \dots (5)$$

and

$$Z = \frac{1.0}{1.5\rho_t \sqrt{\frac{B}{s}}} \dots \dots \dots (6)$$

where A_{co} = area of core measured from center to center of the perimeter tie; A_s = area of longitudinal steel; B = core size measured from center to center or perimeter tie in in.; C = distance between laterally supported longitudinal bars of $4B/n$ in in.; f'_c = cylinder strength of concrete in psi; f_{cp} = strength of unconfined concrete in the column = $K_p f'_c$; f'_s = stress in the lateral steel in psi; K_p = ratio of unconfined concrete strength in the column to f'_c ; n = number of arcs containing concrete that is not effectively confined, also equal to the number of laterally supported longitudinal bars; $P_{occ} = K_p f'_c (A_{co} - A_s)$, unconfined strength of concrete core in kips; s = tie spacing in in.; ρ_t = ratio of the volume of tie steel to the volume of core; and ϵ_0 = strain corresponding to the maximum stress in unconfined concrete. Since the strength of concrete in the specimens, on which the model was based, was in the vicinity of 4,000 psi (28 MPa), (3) produced results that compared well with the test results. A more general equation, suitable for varied concrete strength, was later suggested (Sheikh and Yeh 1982) as follows:

$$\epsilon_{s1} = 0.0022K_s \dots \dots \dots (7)$$

Eq. (7) also makes it possible to use a standard second-degree parabolic equation to represent ascending parts of the curves for both confined and unconfined concrete without affecting initial tangent modulus of elasticity.

Fafitis and Shah (SF) Model

Based on the experimental results of small-diameter (3 in. \times 6 in. [76 mm \times 152 mm]) concrete cylinders, Fafitis and Shah (1985) proposed a set of equations to represent stress-strain curves for confined and unconfined concrete. The slope of the initial tangent of the curve is unaffected by the confinement parameters, and the stress and strain values for peak point are given by the following equations:

$$f'_{cc} = f'_c + \left(1.15 + \frac{3,048}{f'_c} \right) f_r \dots \dots \dots (8)$$

and

$$\epsilon_{cc} = 1.027(10^{-7})f'_c + 0.0296 \frac{f_r}{f'_c} + 0.00195 \dots \dots \dots (9)$$

The units for stress are psi in (8) and (9). The term f_r represents lateral pressure on core concrete. In addition to affecting the peak stress and strain values, lateral pressure f_r also determines the shape of the descending part of the curve as shown by the following equation:

$$f_c = f'_{cc} e^{[-k(\epsilon_c - \epsilon_{cc})^{1.15}]} \dots \dots \dots (10)$$

where

$$k = 0.17f'_c e^{-(0.01f_r)} \dots \dots \dots (11)$$

It was suggested by the authors (Fafits and Shah 1983) of the model, that the model can also be used for columns with rectilinear lateral reinforcement. In the application of the model, square columns were assumed to act as circular columns having an equivalent diameter equal to the side of the confined core. It should be noted that this assumption implies that the distribution of the lateral and longitudinal steel does not affect the lateral pressure and, hence, the behavior of confined concrete.

Model by Mander et al.

Mander et al. (1988) have proposed a unified stress-strain approach for confined concrete that is applicable to both circular and rectilinear transverse reinforcement. The stress-strain curve is based on the equation proposed by Popovics (1973), in which the shape of the descending part of the curve depends upon the secant modulus at the peak point.

To find the confined concrete strength (f'_{cc}), the effective confining pressure was calculated based on the arching of concrete, similar to the one used by Sheikh and Uzumeri (1982) in their model, between layer of hoops in the vertical plane and horizontally between longitudinal bars. Based on the triaxial tests of Schickert and Winkler (1979), the multiaxial failure surface described by William and Warnke (1975) was used in this formulation as suggested by Elwi and Murray (1979). For sections with equal confining pressure in two directions, strength of concrete is given by the following equation:

$$f'_{cc} = f_{co} \left[-1.254 + 2.254 \sqrt{1 + \frac{7.94f'_l}{f'_{co}}} - 2 \frac{f'_l}{f'_{co}} \right] \dots \dots \dots (12)$$

where f'_{co} = unconfined concrete compressive strength; and f'_l = effective lateral confining pressure = $k_e \times$ lateral pressure, and k_e = ratio between effectively confined concrete area and core concrete area.

Strain corresponding to the maximum stress is given by

$$\epsilon_{cc} = \epsilon_{co} \left[1 + 5 \left(\frac{f'_{cc}}{f_{co}} - 1 \right) \right] \dots \dots \dots (13)$$

where ϵ_{co} = strain corresponding to maximum stress in unconfined concrete.

Larger effective confining pressure would result in higher strength and correspondingly higher strain value. Ductility of the concrete as indicated by the postpeak part of the curve will also increase.

APPLICATION OF ANALYTICAL MODELS

Typical confined concrete stress-strain properties for two specimens (A-3 and E-8), as obtained from using different confinement models, are shown in Fig. 2. It is obvious that models by Mander, and Fafitis and Shah predict higher strength and somewhat higher ductility of confined concrete compared with the other models. A similar trend was also observed for other specimens.

A computer program was developed to carry out calculations for theoretical moment-curvature relations of the test specimens using the concrete stress-strain curves from the four analytical models described previously. The required input data included cross-sectional dimensions of specimens, position, and amount of longitudinal steel including the location of laterally supported longitudinal bars, properties of longitudinal steel, stress in tie steel at maximum moment, unconfined concrete strength (f_c), and applied axial load. The section was divided into 40 small slices, each one containing two kinds of elements, core, and cover.

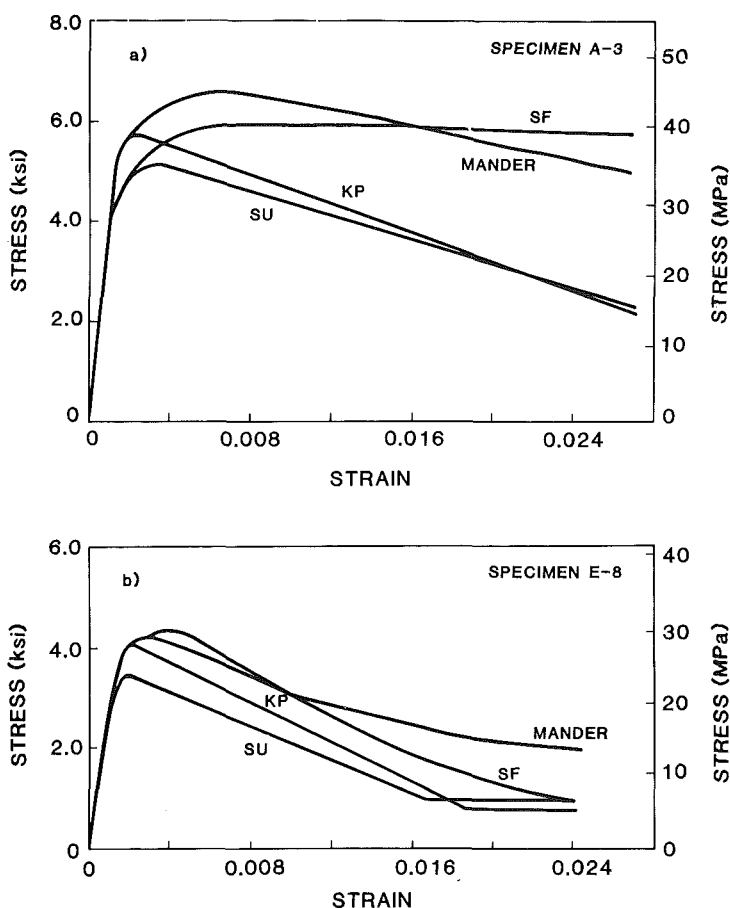


FIG. 2. Analytical Stress-Strain Curves for Confined Concrete

The analysis procedure involved following steps: (1) Assign an initial value of compressive strain at extreme concrete fiber; (2) assume a neutral axis depth; (3) calculate strain at the middle of each element and in longitudinal steel bars; (4) use appropriate stress-strain models for confined and unconfined concrete to determine stress values; (5) calculate axial force and compare with the applied force (If the difference is less than or equal to 0.5%, results are acceptable and moment and curvature values are computed. Otherwise, adjust neutral axis depth and return to step 3. If convergence does not occur in 300 iterations, the program moves to next point), (6) set new concrete strain and return to step 2.

This procedure was continued until the calculated curvature was larger than the maximum measured curvature. In the application of the analytical models, a few assumptions were needed to be made and these are explained here. In three models (Kent and Park, Fafitis and Shah, and Mander et al.), lateral steel stress is suggested to be equal to yield stress. Use of yield stress in these models resulted in unconservative predictions of test results in general. In reality, stress in the ties is gradually developed, and yielding, in most cases, took place in the later part of the test beyond the peak flexural capacity. To reflect this observation, tie stress at maximum moment was used in these models as suggested in the model by Sheikh and Uzumeri (1982). Three models (Fafitis and Shah 1985; Mander et al. 1988; Park et al. 1982) provide stress-strain curves for unconfined concrete along with the curves for confined concrete. In the application of the fourth model (Sheikh and Uzumeri 1982), the plain concrete curve suggested by Kent and Park (1971) was used. In the application of the Sheikh and Uzumeri (SU) (1982) model, the value of K_p was assumed to be equal to 0.85.

The model by Mander et al. (1988) provides a generalized procedure that can take into account path dependence of the concrete loading on its stress-strain relationship. This feature of the model was not used in the analysis for the following reasons. Under the application of the axial load only, the concrete stress in the columns varied between $0.39f'_c$ and $0.65f'_c$. With the addition of flexure, the stress in part of the section increased; while in the rest of the section, the concrete stress was reduced. The increase in the stress was monotonic and the reduction in stress, from a value which was never much higher than $0.5f'_c$, did not produce any significant residual strain or stress in the section. The path dependence of the concrete loading is therefore believed to have no effect on the behavior of specimens in this series of tests.

Comparison of Analytical and Experimental Results

Figs. 3–10 show the comparisons between the moment-curvature relations for eight representative specimens (Sheikh and Yeh 1990) out of a total of 16 tests, and those from the numerical analyses from the four models discussed previously. The model by Mander et al. (1988) consistently overestimated the moment capacities of the sections. The difference between test and analytical moment capacities was found to be about 35% for most of the specimens. This difference is even larger for specimens with lower volumetric ratio of the steel. The Fafitis and Shah model (1985) also overestimated the section capacity in almost all the columns to the same extent as Mander's model did. This is caused by excessively high concrete strength computed from the two models. For this reason, there is a marked difference between the predicted and the experimental curves for the columns tested under high axial loads. For well-confined columns tested under low to me-

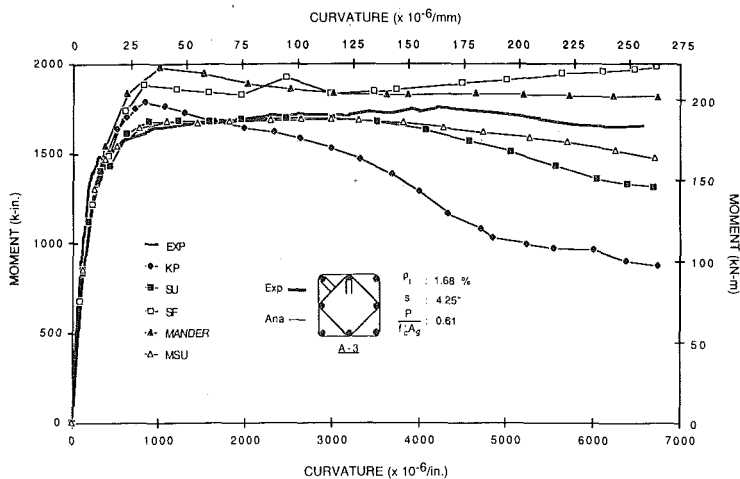


FIG. 3. Comparison of Experimental and Analytical Curves for Specimen A-3

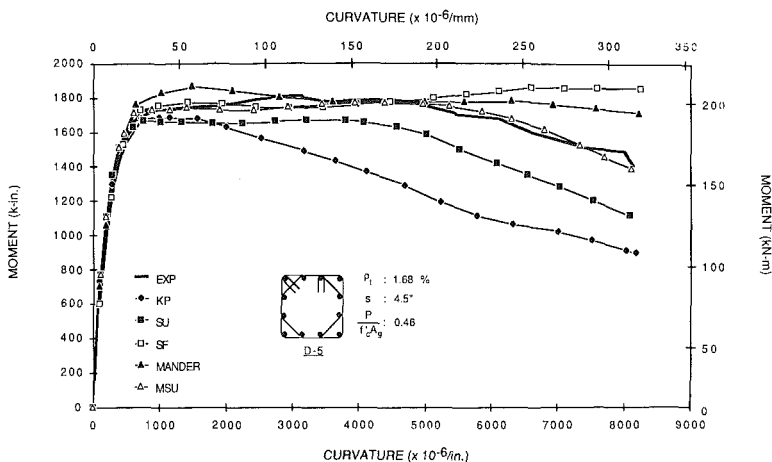


FIG. 4. Comparison of Experimental and Analytical Curves for Specimen D-5

dium axial loads, the predictions from these two models, although mostly unconservative, are reasonable (Figs. 3 and 4). As mentioned earlier, equations for the Shah and Fafitis model were determined from a statistical analysis of the experimental data on 3 in. \times 6 in. (76 mm \times 152 mm) cylinders. The size effect in addition to the type of confinement provided may also be responsible for the large variations between the computed and the test values.

In the application of the model by Mander et al (1988), the strength of unconfined concrete in the specimens (f_{co}) is assumed to be equal to f'_c and ϵ_{co} corresponded to f'_c . For the current series of tests, ϵ_{co} varied between 0.002 and 0.0022. A reduced f_{co} ($=0.85f'_c$ to $0.95f'_c$) in the model would

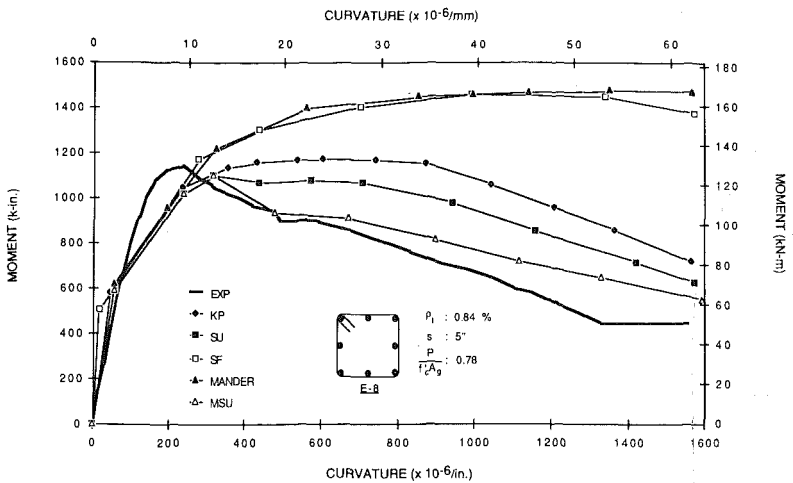


FIG. 5. Comparison of Experimental and Analytical Curves for Specimen E-8

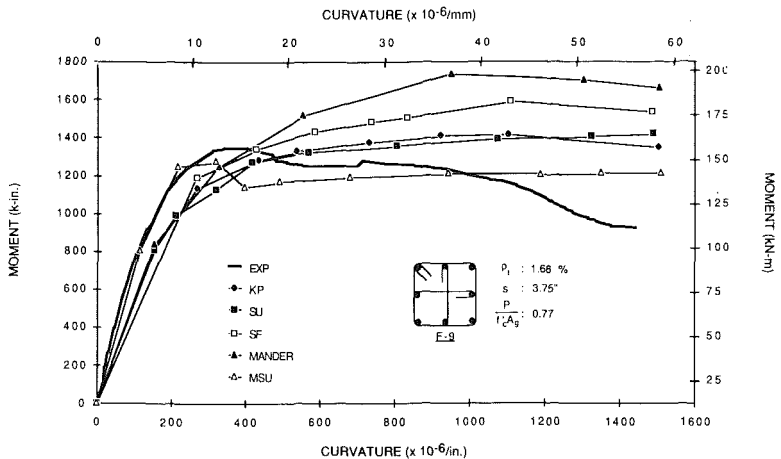


FIG. 6. Comparison of Experimental and Analytical Curves for Specimen F-9

still not accurately predict the behavior of the specimens unless the effect of the volumetric ratio of tie steel is adequately recognized.

Analytical results from the modified Kent and Park model underestimated the sectional capacities for specimens under low to medium axial load levels and overestimated the capacities for specimens under high axial loads. For columns with only four longitudinal bars laterally supported by tie bends, the predictions from this model were worse than those for other columns and were on the unsafe side. The differences between the experimental and the computed moment capacities, however, are much smaller for most columns than as compared with those obtained from Mander, and Shah and Fafitis models. The differences between the computed and the experimental curves at large deformations were quite significant.

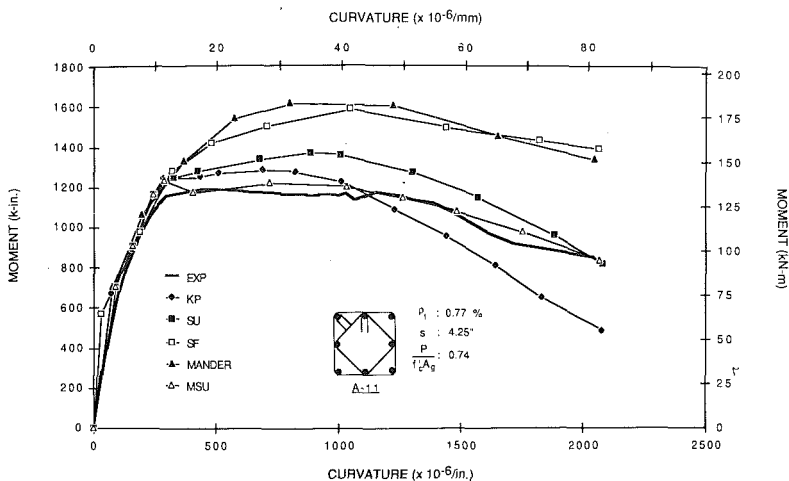


FIG. 7. Comparison of Experimental and Analytical Curves for Specimen A-11

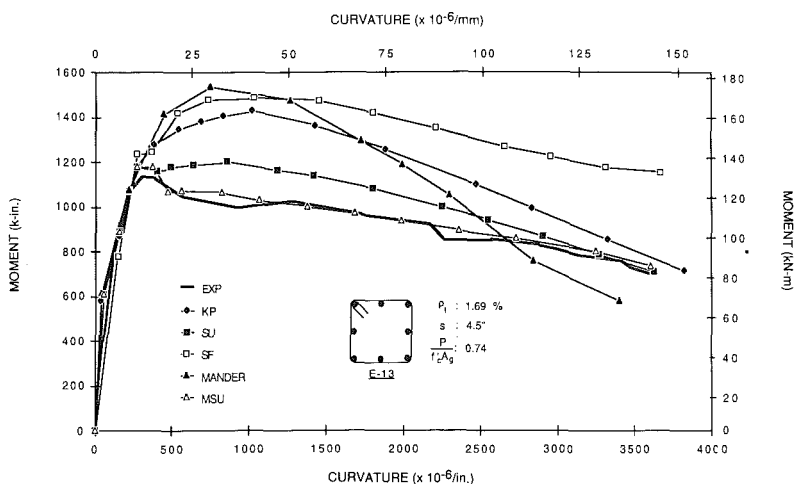


FIG. 8. Comparison of Experimental and Analytical Curves for Specimen E-13

The model by Sheikh and Uzumeri (1982) gave better results than other models, but a consistent effect of the level of axial load was observed on the accuracy of the model. In several cases, this model slightly underestimated column behavior with respect to both strength and ductility. The slopes of the descending portions of the analytical curves were somewhat steeper than the experimental results for most columns. This model was originally calibrated against test data from concentrically loaded specimens. The presence of strain gradient in the specimens appears to be responsible for the lack of accuracy described previously. In addition, a trend was clearly observed that the model overestimated sectional flexural capacities for columns tested under high axial loads. It was felt that by incorporating the

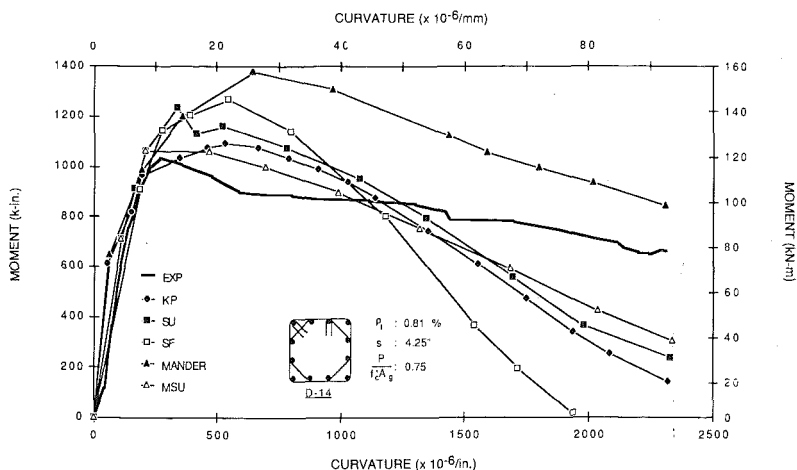


FIG. 9. Comparison of Experimental and Analytical Curves for Specimen D-14

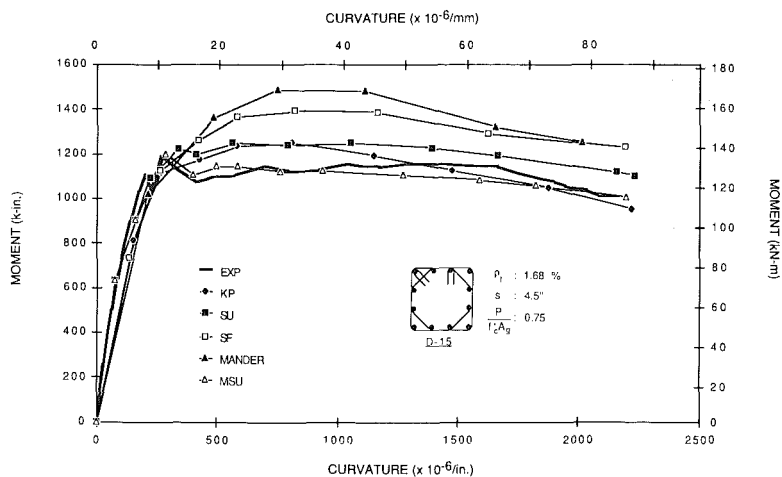


FIG. 10. Comparison of Experimental and Analytical Curves for Specimen D-15

effects of strain gradient and the presence of high axial load along with bending in this model, the required stress-strain curve can be developed.

Modification of Concrete Model

The stress-strain relation of concrete cannot be related to flexural behavior directly. Change in a single parameter in the stress-strain model does not necessarily result in a proportional change in flexural behavior. This complicates the process to investigate the effects of the isolated variables on the behavior of a column. Compared to concentric compression, behavior of concrete under eccentric compression is influenced by several additional variables. Among these are the strain gradient in the section, level of axial

load, and the flexural gradient along the member length. Studies on the effects of strain gradient on the behavior of unconfined concrete have shown conflicting results. Hognestad et al. (1955) concluded, based on their test results, that stress-strain curves under concentric compression (using standard cylinders) and under eccentric compression (using 5×8 in. [127×203 mm] specimens) were very similar. For higher-strength concrete (4,000–5,000 psi [28–35 MPa]), however, the maximum stress reached in the eccentrically loaded specimens was about 93% of the cylinder strength. Sturman et al. (1965) observed that the peak of the curve obtained from the flexural tests was located at a strain 50% higher and a stress about 20% larger than those in the concentrically loaded specimens. Sargin (1971) and Karsan and Jirsa (1969) observed that strain gradient increases the ductility of concrete, but has a negligible effect on its strength.

To include the beneficial effects of strain gradient on ductility in the Sheikh-Uzumeri model, an approach similar to that by Sargin (1971) was used, and (3) was modified to the following equation (Sheikh and Yeh 1982).

$$\frac{\epsilon_{s2}}{\epsilon_o} = 1 + \left\{ \frac{0.81}{C} \left[1 - 5 \left(\frac{s}{B} \right)^2 \right] + 0.25 \sqrt{\frac{B}{c}} \right\} \frac{\rho_t f'_s}{\sqrt{f'_c}} \dots \dots \dots (14)$$

In the determination of the additional term, $0.25 \sqrt{B/c}$, test data from Sargin (1971) and Chan (1955) were used. The additional strain obtained as a result of strain gradient is shown in Fig. 1 as BB'.

The original model developed for concentric compression is based on determining the effectively confined concrete area in a column that is less than the core area. In a section with flexural strain gradient, the fraction of the core area (λ) that is effectively confined varies with the depth of the neutral axis as shown in Fig. 11 for various steel arrangements. For c/B smaller than 0.5, which for most sections indicates low axial load, the λ -value based on concentric compression will overestimate the efficiency of confinement somewhat, but the sectional behavior will not be significantly influenced by a small change in concrete strength. In addition, any possible increase of concrete strength due to a steep strain gradient will compensate for the overestimation of strength due to confinement. For c/B larger than 0.5, when concrete strength significantly influences the sectional behavior,

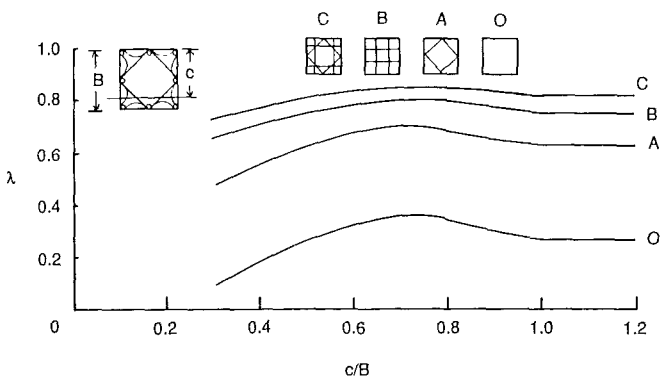


FIG. 11. Influence of Neutral Axis Depth on Confinement Effectiveness

the efficiency of confinement is at least equal to that under concentric compression.

As described earlier, the flexural strength predictions from the model by Sheikh and Uzumeri changed from conservative to unsafe as the axial load increased. Under high axial load, the strength of concrete in flexural compression appears to be less than f'_c in columns with lateral steel contents approximately equal to 50% of the ACI seismic requirements ("Building" 1989). To calculate the strength of confined concrete, an additional factor η was introduced to represent the effect of axial load such that $f'_{cc} = K_s \eta f'_c$. The value of η that produced the best results for flexural strength are plotted in Fig. 12 along with a best-fit line. This line was biased with the introduction of P_b , the balanced load based on the ACI code procedure. A least-squares method was used to develop the following equation for which the mean error was 0.0003. A linear relationship is proposed for simplicity, although a higher-order equation may be more appropriate.

$$\eta = 1 - 0.575 \frac{P - P_b}{f'_c A_g} \leq 1.0 \dots \dots \dots (15)$$

This equation is valid only for the range of axial load studied in this test program. It is clear from Fig. 12 that with an increase in axial load, the strength of concrete in compression is reduced.

As mentioned earlier, slopes of the descending parts of the analytical $M-\phi$ curves were steeper than the test values in most of the specimens. This was investigated by reevaluating the constant 0.225 in (5). The variation of this constant, termed as ξ , is shown in Fig. 13 for the best results for all the columns. The evidence suggests no dependency of ξ on axial load. It should be noted that the original value of ξ (0.225) provides a conservative estimate of ductility and represents the lower bound solution for the specimens tested during this study. A value of 0.29, however, provided more accurate results.

With all the modifications discussed previously, the model was applied to calculate the moment-curvature behavior of all the columns tested during this study. The analytical curves thus obtained (labeled as MSU) are also shown in Figs. 3-10. With the exception of specimen A-16, the analytical and experimental curves agree quite well. It is difficult to explain the lower-than-calculated capacity in the case of specimen A-16. It is possible that the strength of concrete in the cylinder did not correctly represent the strength of plain concrete in this column.

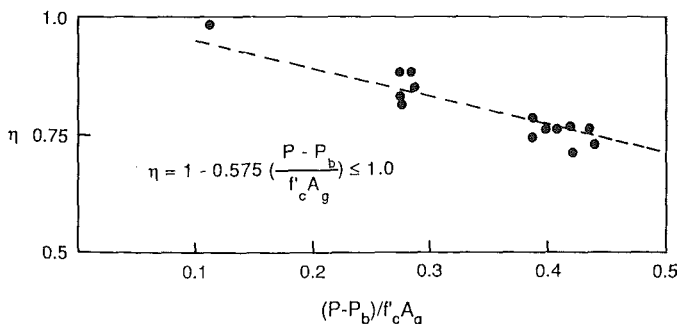


FIG. 12. Variation of η with Axial Load

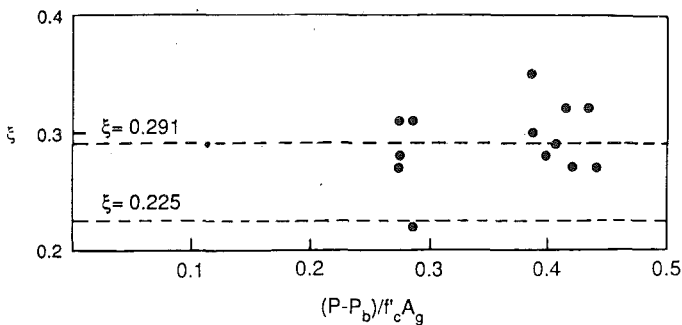


FIG. 13. Variation of ξ with Axial Load

Equivalent Rectangular Stress Block

To simplify the application of the proposed stress-strain model in flexure, equivalent stress block with dimensions $\beta f'_{cc}$ and $\alpha \epsilon_{cc}$ was developed (Sheikh and Yeh 1982). The resulting equations for α and β along with a numerical example are given in the following.

To generalize the procedure, the following three parameters are introduced, $\Omega = \epsilon_c/\epsilon_{s1}$ and $D = \epsilon_c/\epsilon_{s2}$ and $G = \epsilon_c/\epsilon_{s85}$, where ϵ_c is the extreme fiber concrete strain and ϵ_{s1} , ϵ_{s2} and ϵ_{s85} are defined in Fig. 1. Values of α and β are calculated as follows.

- Region 1: ($\epsilon_c \leq \epsilon_{s1}$)

$$\alpha = \frac{4 - \Omega}{2(3 - \Omega)} \dots \dots \dots (16)$$

and

$$\beta = \frac{2\Omega(3 - \Omega)^2}{3(4 - \Omega)} \dots \dots \dots (17)$$

- Region 2: ($\epsilon_{s1} < \epsilon_c \leq \epsilon_{s2}$)

$$\alpha = \frac{6\Omega^2 - 4\Omega + 1}{2\Omega(3\Omega - 1)} \dots \dots \dots (18)$$

and

$$\beta = \frac{2(3\Omega - 1)^2}{3(6\Omega^2 - 4\Omega + 1)} \dots \dots \dots (19)$$

- Region 3: ($\epsilon_{s2} < \epsilon_c \leq \epsilon_{s30}$) (ϵ_{s30} is the strain at $f_c = 0.3f'_{cc}$)

$$\alpha\beta = 1 - \frac{1}{3\Omega} - 0.075 \left(\frac{GD}{D - G} \right) \left(1 - \frac{1}{D} \right)^2 \dots \dots \dots (20)$$

$$\alpha = 2 - \frac{1}{\alpha\beta} \left[1 - \frac{1}{6\Omega^2} - \frac{G(2D^3 - 3D^2 + 1)}{20D^2(D - G)} \right] \dots \dots \dots (21)$$

Example

Specimen A-3, with core dimensions and material properties as given in Fig. 14, is subjected to 300 kips (1,334 kN) of axial load. What is the ultimate moment capacity of the section if the ultimate strain (ϵ_u) in the core is 0.0075?

The controlling parameters K_s , ϵ_{s1} , ϵ_{s2} , and ϵ_{s85} can be calculated with $B = 10.5$ in., $C = 4.688$ in., $\rho_s = 0.0168$, and $f'_s = 70.8$ ksi. From the ACI Code procedure, $P_b = 210$ kips. Using (15), $\eta = 0.923$. $P_{occ} = 0.923(4.67)(10.5^2 - 3.52) = 460.1$ kips. From (2)

$$K_s = 1.0 + \frac{(10.5)^2}{(10.58)(460.1)} \left\{ \left[1 - \frac{8(4.688)^2}{5.5(10.5)^2} \right] \left[1 - \frac{3.75}{2(10.5)} \right]^2 \right\} \sqrt{(0.168)(70,800)} = 1.342 \dots (22)$$

Therefore, $f'_{cc} = (0.923)(1.342)(4.67) = 5.785$ ksi. From (3)

$$\epsilon_{s1} = 0.00345 \dots (23)$$

From (4)

$$\epsilon_{s2} = 0.00418 + (0.0282)/\sqrt{c} \dots (24)$$

Assuming that $\epsilon_{s2} \geq 0.0075$, the stress and strain distribution are shown in Fig. 15.

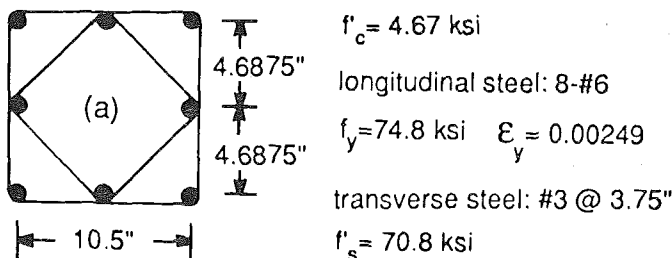


FIG. 14. Section of Example and Material Properties

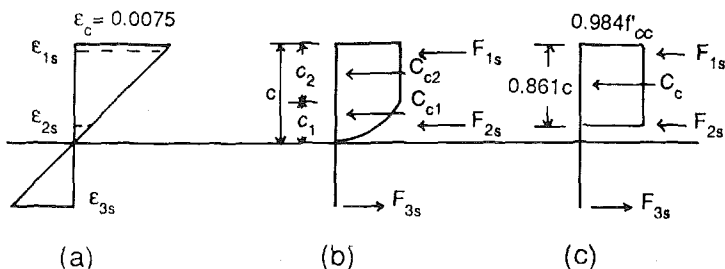


FIG. 15. Strain and Stress Distribution

The parameters for equivalent stress blocks for region 2 [(18) and (19)] are

$$\Omega = \frac{\epsilon_c}{\epsilon_{s1}} = \frac{0.0075}{0.00345} = 2.174 \quad \dots \dots \dots (25)$$

$$\alpha = \frac{6\Omega^2 - 4\Omega + 1}{2\Omega(3\Omega - 1)} = 0.861 \quad \dots \dots \dots (26)$$

$$\beta = \frac{2(3\Omega - 1)^2}{3(6\Omega^2 - 4\Omega + 1)} = 0.984 \quad \dots \dots \dots (27)$$

Assuming that top and bottom steel have yielded, the equilibrium equation can be written as

$$P = C_c + F_{2s} = 300 \quad \dots \dots \dots (28)$$

or

$$\alpha\beta(f'_{cc})(B)(c) + \frac{c - 5.25}{c} (\epsilon_c)(E_s)(A_{2s}) = 300 \quad \dots \dots \dots (29)$$

Solve for $c = 5.59$ in. (for $c/B = 0.53$, effect of location of neutral axis can be ignored).

Both ϵ_{1s} and ϵ_{2s} are greater than ϵ_y . Forces in steel and concrete are given as: compression $F_{1s} = 99$ kips, $F_{2s} = 12$ kips, $C_c = 288$ kips; and tension $F_{3s} = 99$ kips. Moment about plastic centroid is given by $M = 288[5.25 - (0.5)(.861)(5.59)] + 2(99)(4.688) = 1,743$ kips-in.; $\phi = 0.0075/5.59 = 0.00134$ radians/in.

SUMMARY AND CONCLUSIONS

Work reported in this paper is a follow-up of the experimental research reported earlier. Several available stress-strain models for confined concrete were briefly reviewed and used to predict the moment-curvature behavior of the specimens tested as part of this research program. Most of the models resulted in inaccurate predictions because they did not consider all the variables investigated in this study.

The model proposed by Sheikh and Uzumeri (1982), originally developed for concentric compression, was modified to reflect the effects of strain gradient and the level of axial load. The analytical results for both the original model and from the modified version are presented in this paper. There is no convincing experimental evidence that strain gradient enhances strength of concrete. The effect of strain gradient on the fraction of the core area that is effectively confined is also not significant. The major changes in the model reflect enhanced ductility due to strain gradient and the dependence of the concrete strength on the level of axial load. Above the balanced load level, strength of concrete reduces with an increase in axial load. A linear variation is suggested for convenience for the range of axial load tested, although a higher-order equation may be more appropriate.

Although the original model predicted the moment-curvature behavior of the confined concrete sections under axial load and flexure quite well, the modified model resulted in more accurate representations of the experimental results.

ACKNOWLEDGMENTS

Research reported here was supported by grants from the National Science Foundation and the Texas Advanced Technology Research Program.

APPENDIX. REFERENCES

- "Building code requirements for reinforced concrete." (1989). *ACI 318-89*, American Concr. Inst., Detroit, Mich.
- Chan, W. W. L. (1955). "The ultimate strength and deformation of plastic hinges in reinforced concrete frameworks." *Mag. Concr. Res.*, 7(21), 121-132.
- Elwi, A. A., and Murray, D. W. (1979). "A 3D hypoelastic concrete constitutive relationship." *J. Engrg. Mech. Div.*, ASCE, 105(4), 623-641.
- Fafitis, A., and Shah, S. P. (1985). "Predictions of ultimate behavior of confined concrete columns subjected to large deformations." *ACI J.*, 82(4), 423-433.
- Fafitis, A., and Shah, S. P. (1983). "Discussion of 'A comparative study of confinement models.'" *ACI J.*, 80(3), 261-263.
- Hognestad, E., Hanson, N. W., and McHenry, D. (1955). "Concrete stress distribution in ultimate strength design." *ACI J.*, 52(4), 455-480.
- Karsan, I. D., and Jirsa, J. O. (1969). "Behavior of concrete under compressive loading." *Proc., J. Struct. Div.*, ASCE, 95(12), 2543-2563.
- Kent, D. C., and Park, R. (1971). "Flexural members with confined concrete." *J. Struct. Div.*, ASCE, 97(7), 1969-1990.
- Mander, J. B., Priestley, M. J. N., and Park, R. (1988). "Theoretical stress-strain model for confined concrete." *J. Struct. Engrg.*, ASCE, 114(8), 1804-1826.
- Park, R., Priestley, M. J. N., and Gill, W. D. (1982). "Ductility of square confined concrete columns." *J. Struct. Div.*, ASCE, 108(4), 929-950.
- Paulay, T. (1980). "Deterministic design procedure for ductile frames in seismic areas." *ACI Special Publication No. SP63: Reinforced concrete structures subjected to wind and earthquake forces*, American Concrete Institute, Detroit, Mich., 357-381.
- Popovics, S. (1973). "A numerical approach to the complete stress-strain curves for concrete." *Cem. Concr. Res.*, 3(5), 583-599.
- Sargin, M. (1971). "Stress-strain relationships for concrete and the analysis of structural concrete sections." *Study No. 4*, Solid Mech. Div., Univ. of Waterloo, Waterloo, Ontario, Canada.
- Schickert, G., and Winkler, H. (1979). *Results of tests concerning strength and strain of concrete subjected to multiaxial compressive stresses*. Deutscher Ausschuss für Stahlbeton, Berlin, West Germany, Heft 277.
- Sheikh, S. A. (1982). "A comparative study of confinement models." *ACI J.*, 79(4), 296-306.
- Sheikh, S. A., and Uzumeri, S. M. (1982). "Analytical model for concrete confinement in tied columns." *J. Struct. Div.*, ASCE, 108(12), 2703-2722.
- Sheikh, S. A., and Yeh, C. C. (1982). "Flexural behavior of confined concrete columns." *ACI J.*, 83(3), 389-404.
- Sheikh, S. A., and Yeh, C. C. (1990). "Tied concrete columns under axial load and flexure." *J. Struct. Engrg.*, ASCE, 116(10), 2780-2800.
- Sturman, G. H., Shah, S. P., and Winter, G. (1965). "Effect of flexural strain gradient on microcracking and stress-strain behavior of concrete." *ACI J.*, 62(7), 805-822.
- William, K. J., and Warnke, E. P. (1975). "Constitutive model for the triaxial behavior of concrete." *Proc., Int. Association for Bridge and Struct. Engrg.*, Int. Association for Bridge and Struct. Engrg., 19, 1-30.
- Yeh, C.-C., and Sheikh, S. A. (1988). "Behavior of confined concrete columns under axial load and flexure." *Res. Report No. UHCE 88-2*, Univ. of Houston, Houston, Tex.